

Near threshold photoproduction of η mesons from ^4He

V. Hejny^{1,a}, P. Achenbach^{1,b}, J. Ahrens², R. Beck², S.J. Hall⁴, M. Kotulla¹, B. Krusche¹, V. Kuhr³, R. Leukel², V. Metag¹, R. Novotny¹, V. Olmos de León², R.O. Owens⁴, F. Rambo³, A. Schmidt², M. Schumacher³, U. Siodlaczek⁵, H. Ströher^{1,a}, F. Wissmann³, J. Weiß¹, M. Wolf¹

¹ II. Physikalisches Institut, Universität Gießen, D-35392 Gießen, Germany

² Institut für Kernphysik, Universität Mainz, D-55099 Mainz, Germany

³ II. Physikalisches Institut, Universität Göttingen, D-37073 Göttingen, Germany

⁴ Department of Physics and Astronomy, University of Glasgow, Glasgow G128QQ, UK

⁵ Physikalisches Institut, Universität Tübingen, D-72076 Tübingen, Germany

Received: 24 March 1999 / Revised version: 28 June 1999

Communicated by Th. Walcher

Abstract. Photoproduction of η mesons from ^4He has been measured for the first time. The experiment was performed at the Mainz Microtron (MAMI) using the TAPS photon spectrometer and the Glasgow/Mainz tagged photon facility. η mesons were identified in coincidence with recoil nucleons. Total and differential cross sections are presented in the photon energy range between threshold and 818 MeV. The exclusive data are used to determine the ratio of the elementary production cross sections on bound neutrons and protons, $\sigma_n/\sigma_p = 0.68 \pm 0.02 \pm 0.09$. In addition, upper limits for the total coherent cross section have been derived.

PACS. 13.60.Le Meson production – 14.20.Gk Baryon resonances with S=0 – 14.40.Aq π, K and η mesons – 25.20.Lj Photoproduction reactions – 27.10.+h $A \leq 5$

1 Introduction

Photoproduction of η mesons has recently become an important tool to study the properties of the $S_{11}(1535)$ nucleon resonance. The η is a selective probe for this $I=1/2$ resonance like the pion in the regime of the $\Delta(1232)$. In the threshold region excitation of the S_{11} is the dominant process for η meson production.

This situation is reflected by the experimental program of the TAPS and A2 collaborations at the Mainz Microtron. The study of η photoproduction covered the range from the elementary processes on proton and neutron (the latter by using a liquid deuterium target) [1,2] to the properties of the η meson and the S_{11} resonance in nuclear matter by using complex nuclei [3]. While all these experiments were inclusive measurements in the sense that only the η mesons were detected, the new TAPS setup built in spring 1995 included a dedicated forward wall to identify the recoil nucleon (proton, neutron) or light nucleus (deuteron). This offered the possibility of distinguishing between reactions on protons, neutrons and recoil nuclei directly event by event.

This experimental improvement is important for attempts to unravel the isospin structure of the S_{11} resonance, which is still not unambiguously determined. The isoscalar and isovector amplitudes (A_s, A_v) of the transition $\gamma N \rightarrow \eta N$ are related to the elementary cross sections in the following way:

$$\begin{aligned}\sigma_p &\propto (A_s + A_v)^2 \\ \sigma_n &\propto (A_s - A_v)^2\end{aligned}\quad (1)$$

The coherent cross section on the deuteron ($I=0$), however, only depends on the isoscalar part:

$$\sigma_{d,coh} \propto (A_s)^2 \quad (2)$$

From previous inclusive TAPS measurements [2] a ratio of the isovector to isoscalar part of the transition amplitude of

$$\frac{A_v}{A_s} = 10 \pm 2.5 \quad (3)$$

was extracted. Recent experiments at ELSA [4] verified this ratio and, additionally, determined the coherent cross section on the deuteron in agreement with the TAPS upper limit. The absolute value for the coherent cross section measured at ELSA, however, is still by a factor of 5 larger than calculations based on the isoscalar amplitude extracted from the the proton and neutron data [5].

^a Present address: Institut für Kernphysik, Forschungszentrum Jülich, D-52425 Jülich, Germany

^b Present address: Institut für Kernphysik, Universität Mainz, D-55099 Mainz, Germany

Consequently, improved exclusive experiments are needed. In principle, the ELSA measurement was such an exclusive experiment. The η mesons were detected by their two gamma decay and the recoil nucleons and nuclei were identified using a detector at forward angles. However, due to the limitations of the statistics and the invariant mass resolution of the photon detector (see [4]) the identification of the processes was mainly based on the recoil particle information.

The new TAPS setup was designed to do both the reconstruction of the η meson using an invariant mass analysis and the identification of the recoil particles. It was used to measure η photoproduction from ${}^4\text{He}$ (discussed in this paper) and from the deuteron. The latter experiment will give an additional set of data for the quasifree and coherent mechanisms on the deuteron. The investigation of ${}^4\text{He}$ was carried out not only to determine the ratio of σ_n and σ_p , but also to have an intermediate step from the lightest nuclei to more complex systems.

An additional interesting topic is the coherent production process of η mesons from ${}^4\text{He}$. Due to the quantum numbers of ${}^4\text{He}$ ($S=0$, $I=0$) the production mechanism involving the $S_{11}(1535)$ resonance should be strongly suppressed by angular momentum conservation and no longer dominant. Here, other processes have to be taken into account like the production via the $D_{13}(1520)$ resonance or vector meson exchange. Unfortunately, the present experiment can only provide upper limits for the coherent cross section.

2 Instrumentation and methods

2.1 Experimental setup

The experiment was performed at the Mainz Microtron (MAMI, [6]) using the Glasgow/Mainz tagged photon facility [7] and the photon spectrometer TAPS [8]. The combination of the continuous wave electron accelerator and the tagging facility offers an excellent experimental environment, providing a quasimonochromatic photon beam with a maximum energy of $E_\gamma = 818$ MeV. The energy resolution of the tagging spectrometer is about 2 MeV in the range between the reaction thresholds ($E_\gamma \approx 587$ MeV and ≈ 608 MeV for the coherent and quasifree process, respectively) and the maximum photon energy. The average available photon flux is about 500 kHz/(2 MeV) in the region of interest.

The liquid ${}^4\text{He}$ target cell was 10 cm long and 3 cm in diameter. It was mounted in a scattering chamber of carbon fibre (ϕ 90 cm) to minimize scattering, conversion and energy loss between target and detector.

The η mesons produced were detected by the photon spectrometer TAPS exploiting their decay into two gammas. TAPS is a modular detector system built of single BaF_2 crystals with hexagonal shape. Each crystal is 25 cm long and has an inner diameter of 6 cm. For this experiment the modules were arranged in 6 blocks using an 8x8 geometry and one hexagonal forward wall with 120 modules. The setup used is shown schematically in Fig. 1. To

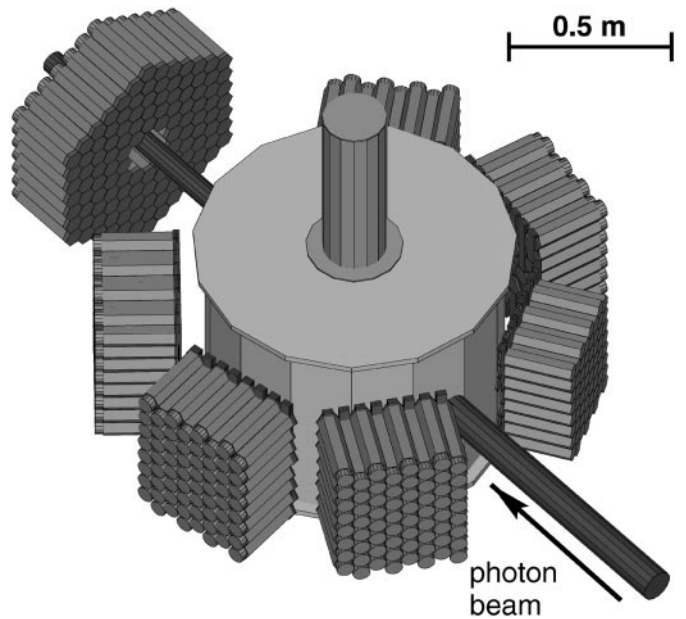


Fig. 1. The detector setup visualized with the GEANT simulation package. The six BaF_2 blocks and the forward wall are arranged around the scattering chamber containing the ${}^4\text{He}$ target. The photon beam comes from the lower right corner

discriminate between charged and neutral particles, the blocks had individual plastic scintillators as veto detectors in front of each module. In addition, the different excitation of the fast and slow components of the BaF_2 scintillation light by different types of particles was used to obtain pulse shape identification as shown in Fig. 2a. In the forward wall this was extended to distinguish light charged particles (π^+ , p, d, ...) photons and neutrons by gluing a fast plastic scintillator on the front surface of the BaF_2 crystal. Both were optically coupled and the light output was read out by the same photomultiplier tube. The so-called phoswich modules worked like a ΔE -E-telescope (Fig. 2b). For further information see [9].

2.2 Data analysis

The photon and particle identification is based on the reconstruction of events in the BaF_2 arrays. Normally a photon produces an electromagnetic shower, which triggers several neighbouring detector modules at a common time, whereas a massive particle deposits energy in just one or two modules. With this information together with that from the veto detectors and the pulse shape analysis mentioned above, an event can be assigned to a physical particle. The impact position of the particle is determined by an energy weighted sum of the single detector locations [10]. While this works for all particle types, the sum of the deposited energies can be used as the particle energy only for photons, for which an energy calibration was carried out using the detection of cosmic radiation [11]. For protons and neutrons different methods have to be applied as discussed below.

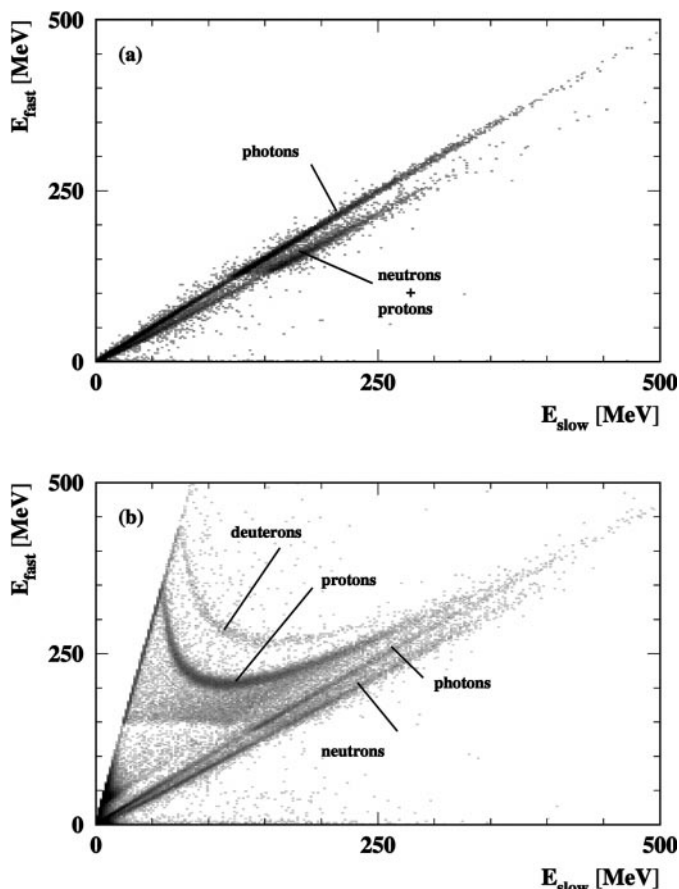


Fig. 2. Two dimensional pulse shape spectra for a BaF₂ module (a) and a forward wall phoswich detector (b). The light output of the fast component is plotted versus the light output of the slow component. Different particle types can clearly be identified

Once the photons are identified, η mesons can be reconstructed using the invariant mass of two coincident photons:

$$\begin{aligned} m_{\gamma\gamma}^2 &= (E_{\gamma_1} + E_{\gamma_2})^2 - (\mathbf{p}_{\gamma_1} + \mathbf{p}_{\gamma_2})^2 \\ &= 2E_{\gamma_1}E_{\gamma_2}(1 - \cos\theta_{\gamma_1\gamma_2}), \end{aligned} \quad (4)$$

where E_{γ_i} and \mathbf{p}_{γ_i} are the energy and momentum of the photons and $\theta_{\gamma_1\gamma_2}$ is the opening angle between them. The result of such an analysis is shown in Fig. 3a. Events with $m_{\text{inv}} > 500$ MeV are processed as η mesons in the subsequent analysis. The time of the η (i.e. the coincidence time of the two photons) is used as an event by event time base to exploit the good time resolution of the TAPS detector ($\sigma_{\text{BaF}_2} = 150$ ps).

As mentioned above, the situation is more complicated for protons: the energy response of the BaF₂ modules is different and the energy loss between reaction vertex and detector has to be taken into account. Since the identical setup has been used to study the single π^0 photoproduction from the proton, this provides the opportunity to calibrate the energy of the protons with energy loss and analysis cuts already included. With the identification of

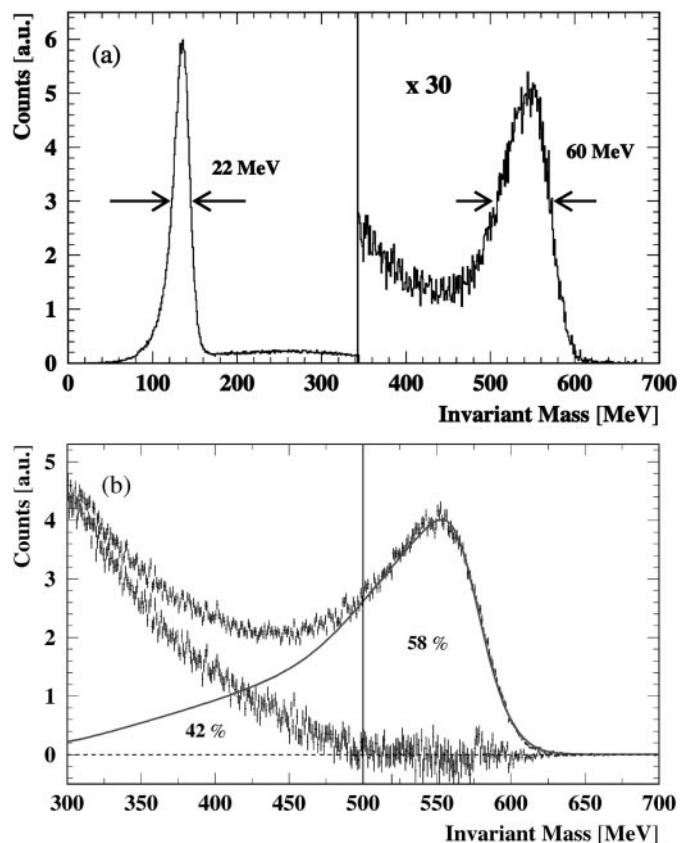


Fig. 3. (a) The two photon invariant mass spectrum obtained in this experiment. It consists of three components: the pion peak at 135 MeV, the η peak at 547 MeV and a smooth combinatorial background from multi pion events (direct two pion production and $\eta \rightarrow 3\pi^0$ decay). (b) The detector response (invariant mass) extracted from GEANT simulations compared with the data. The solid curve represents the shape of the detector response according to GEANT, the upper data set the invariant mass spectrum measured and the lower data set the difference between the experiment and GEANT. Above the analysis cut of $m_{\gamma\gamma} = 500$ MeV no background is left in the data within the statistical error, but 58% of the η decay events are accepted

the π^0 this reaction is kinematically fully determined and the energy and momentum of the outgoing proton can be deduced. This information together with the corresponding energy signals from the TAPS modules determines the calibration.

In case of the neutrons there is no energy loss on the way to the detector, but there is no direct correlation between the energy response of the detector and the kinetic energy of the neutron. Therefore, the time-of-flight-information has been used to extract the neutron kinetic energy. Due to the limited flight path the energy resolution is not as good as for photons and protons.

2.3 Efficiency corrections

To calculate the detector efficiency for η mesons the simulation package GEANT has been used. The ability of

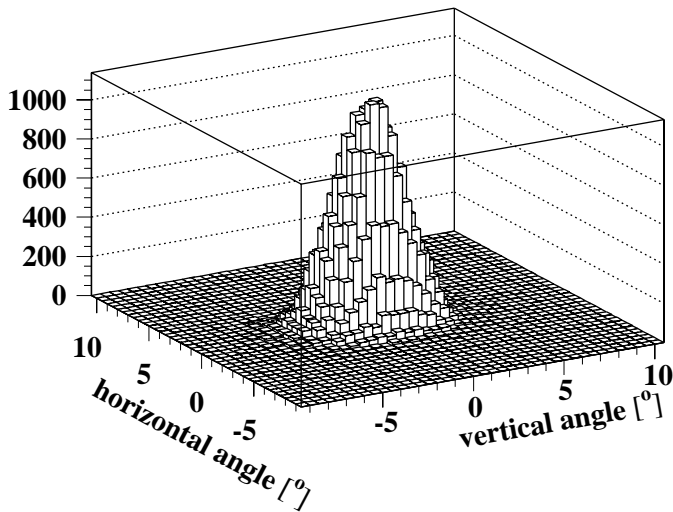


Fig. 4. The angular correlation between a reconstructed and measured proton in the calibration reaction $p(\gamma,\pi^0)p$. FWHM of the distribution is 4 degrees in both directions

this code to describe the detector response of TAPS for photons has previously been demonstrated [12]. As an example the invariant mass spectrum for this experiment is shown in Fig. 3b. In this picture one can see the data compared with the simulation for $m_{\gamma\gamma} > 300$ MeV. The analysis cut for the η mesons has been chosen in such a way that no background is left in the η region. The overall efficiency has been calculated as a function of energy and polar angle of the η mesons. It is typically about 4-5 %.

The proton efficiency was extracted using the energy calibration data (see above) by checking for each kinematically reconstructed proton whether a proton was detected at the predicted location in the TAPS array (within a reasonable uncertainty). As an example Fig. 4 shows the angular correlation between the reconstructed and measured position.

The neutron efficiency was calculated in a similar way [13] using the reaction $\gamma(p,\pi^0\pi^+)n$. The experimentally less difficult reaction $\gamma(p,\pi^+)n$ could not be used because of the kinematical correlation of π^+ and neutron. The efficiency, which is only available for the forward wall, includes the analysis cuts and is shown in Fig. 5.

The relative uncertainties of the extracted overall efficiencies are about 1 % for photons and 5 % for protons and neutrons, respectively.

3 Results

3.1 Inclusive data

In this section the results for the inclusive η photoproduction from ${}^4\text{He}$ are presented. Figure 6 shows the total cross section versus the incident photon energy. The data are compared to a kinematical model in impulse approximation which takes into account the elementary cross section on the proton [1] and the Fermi momentum distribution

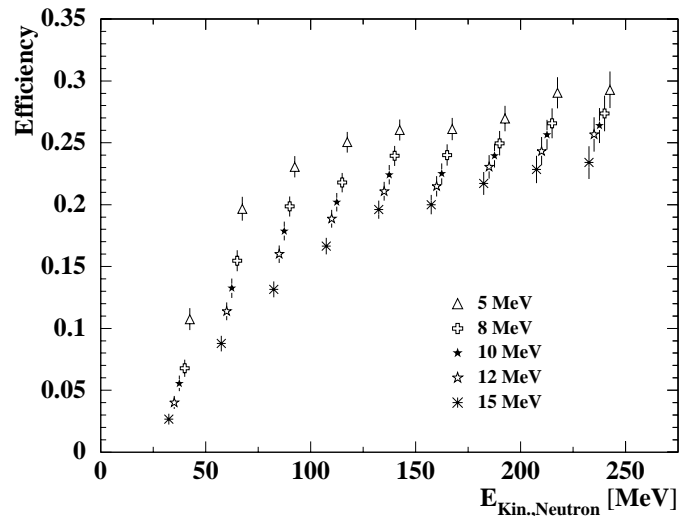


Fig. 5. The energy dependent neutron efficiency (including all analysis cuts) obtained from the reaction $p(\gamma,\pi^0\pi^+)n$ [13]. The different symbols represent different detector thresholds for the deposited energy

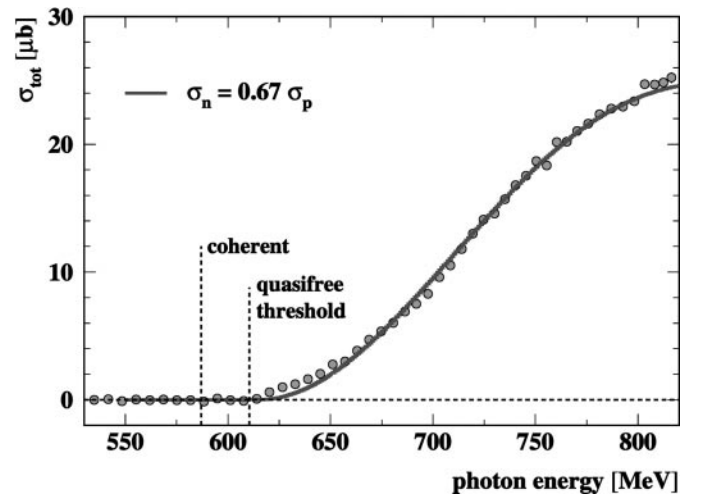


Fig. 6. The total inclusive cross section for η photoproduction from ${}^4\text{He}$. The data are compared to a fit with the participant-spectator model described in the text

in ${}^4\text{He}$ [14]. For a first comparison to the data the cross section on the neutron (σ_n) is assumed to be $0.66 \cdot \sigma_p$ as derived from a former experiment with TAPS on the deuteron [2], where the same model was able to describe the data successfully. Final state interactions between the η meson, the participant nucleon and the spectator nucleus (${}^3\text{H}$, ${}^3\text{He}$) are not taken into account, although they might not be negligible for the strongly bound complex nucleus ${}^4\text{He}$. The total inclusive cross section is reproduced within this simple approach without invoking any η absorption in ${}^4\text{He}$. This does not exclude η rescattering processes which change the kinematic distributions but do not reduce the total η yield. Treating σ_n/σ_p as a free parameter, a best fit to the total cross section yields a cross

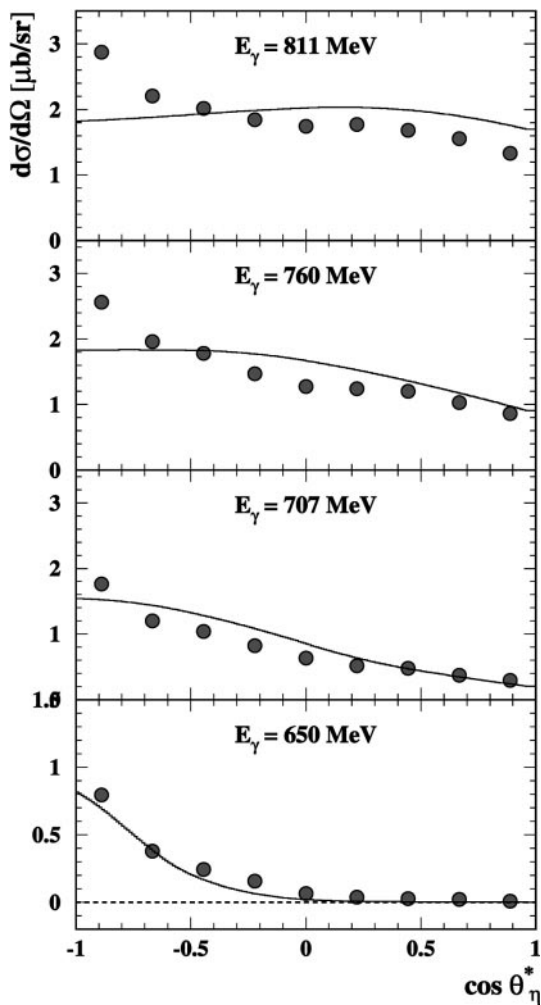


Fig. 7. Angular distributions for inclusive η photoproduction from ${}^4\text{He}$ at four different incident photon energies. The reference frame is the photon-nucleus-c.m.-system. The curves correspond to the predictions of the participant-spectator model

section ratio of

$$\frac{\sigma_n}{\sigma_p} = 0.67 \pm 0.01 \quad (5)$$

The error given is only statistical. The systematic error is strongly linked to the model assumptions. The consistency of the ratio extracted from ${}^2\text{H}$ and ${}^4\text{He}$ data corroborates the neglect of η absorption for these light nuclei in contrast to more complex nuclei [3].

As mentioned above, final state interactions should be observable in kinematic spectra like the angular distribution of the η mesons or recoil nucleons. In Fig. 7 these differential cross sections are shown for four different bins in the incident photon energy. Again, the data points are compared with the model above and one can see significant deviations. This is important because if this model is not able to describe the process kinematics, it cannot be used to extrapolate the exclusive η -nucleon data to the full solid angle. Therefore the cross sections given in the next section are only valid within the detector acceptance.

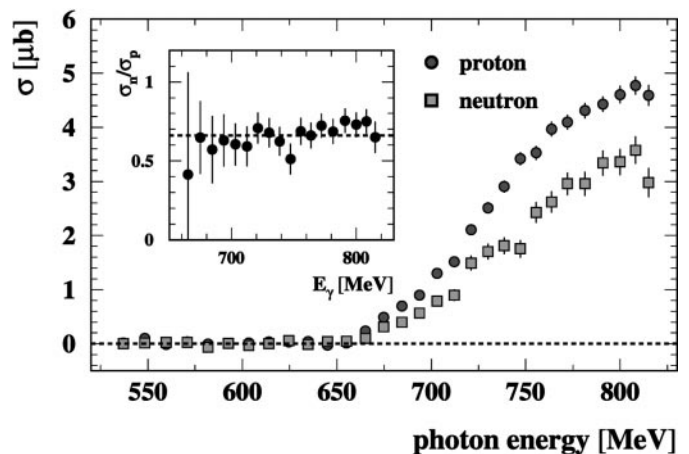


Fig. 8. The exclusive η photoproduction cross section on ${}^4\text{He}$ within the acceptance of the detector setup (see text). The inset shows the ratio of the two data sets

3.2 Exclusive data

In the last section the ratio σ_n/σ_p was extracted from the inclusive total cross section. However, the best way to obtain this ratio is to determine event by event which nucleon (proton or neutron) was the participant in the reaction. For this purpose the additional TAPS forward wall was built. Due to energy losses proton detection was only possible for kinetic energies above $E = 60$ MeV. Since proton and neutron emission in coincidence with an η meson have to be compared, this limit must also be applied to neutrons.

In Fig. 8 the cross sections within $\sigma_{\text{acc},n}$ and $\sigma_{\text{acc},p}$ above this energy limit and within the $5^\circ - 19^\circ$ polar angle acceptance of the forward wall are presented. The inset shows the ratio between the two data sets. There is no significant energy dependence in the energy range covered. The mean value is

$$\frac{\sigma_n}{\sigma_p} = 0.68 \pm 0.02 \pm 0.09. \quad (6)$$

The errors given are statistical and systematic, respectively. The systematic error is mainly due to the uncertainty of the nucleon detection efficiencies, the error caused by the influence of final state interactions is not taken into account. As stated in the last section, the comparison of the results from deuterium and ${}^4\text{He}$ indicates that η -rescattering effects are not important for the inclusive cross section. Their influence on the cross section ratio derived from the exclusive data must even be smaller since η -mesons produced on a proton or on a neutron will be effected in a similar way. The exclusive measurement could be influenced by nucleon charge exchange rescattering but this effect has no impact on the inclusive data. The very good agreement between the inclusive and exclusive results therefore strongly suggests that such effects are not important.

The same cross section ratio can be deduced from the nucleon energy spectra integrated over the available photon energy range (Fig. 9a). The experimental cross sec-

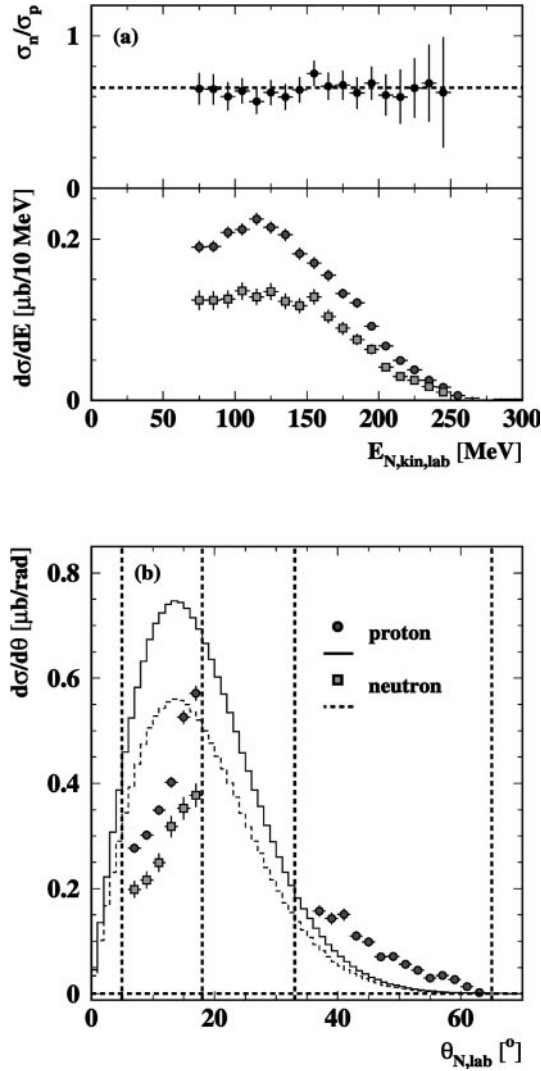


Fig. 9. (a) The appropriate kinetic energy differential cross sections of the recoil nucleons for η photoproduction from ${}^4\text{He}$ within the detector acceptance together with the ratio of the two data sets. (b) The angular differential cross section compared with the output of the participant-spectator model (solid and dashed histograms, respectively). The vertical dashed lines indicate the angular range subtended by the forward wall and the two most forward TAPS blocks

tion ratio, now derived in inclusive and exclusive measurements, can be compared to quark model predictions [15–20] which are in the range of $\sigma_n/\sigma_p = 0.4 - 1.1$.

To corroborate the statement of the last section, that the model used to describe the inclusive data is not able to give a full kinematical description of the process, the angular distribution of the nucleons is shown in Fig. 9b. For the protons the TAPS block data are also included in this spectrum. The two curves represent the model predictions for protons and neutrons, respectively. As one can see the data are much more backward peaked than the calculation. Unfortunately, there is no more elaborate model for quasifree η photoproduction from ${}^4\text{He}$.

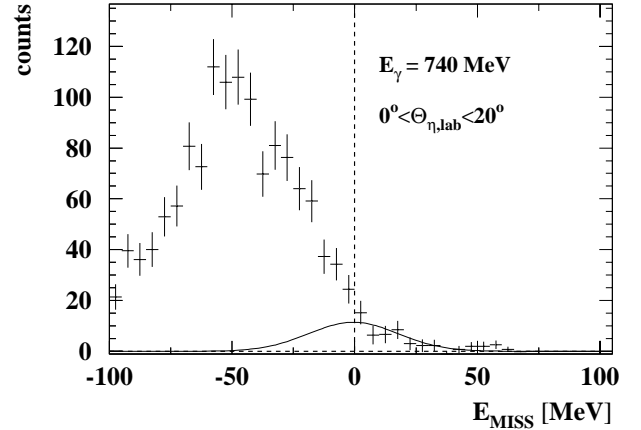


Fig. 10. Missing energy spectrum assuming coherent production kinematics. The solid curve represents a fit to the data with $E_{\text{MISS}} > 0$ for a coherent signal folded with the detector response; it is taken as an upper limit for the yield of coherent events

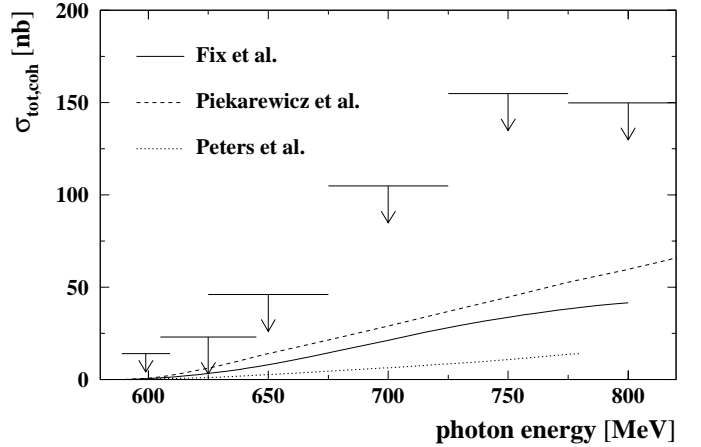


Fig. 11. The extracted upper limits for coherent η photoproduction from ${}^4\text{He}$ versus the incident photon energy. Three theoretical predictions are included for comparison [21–23]

3.3 Coherent η production

In contrast to the quasifree mechanism coherent photoproduction is a theoretically well explored field. The calculations [21–23] all predict that the cross section is near or below the detection limit of this experiment. Since there was no satisfactory model for the quasifree cross section, the task of distinguishing the coherent events from the quasifree background could not be as sensitive as necessary. To illustrate the situation, Fig. 10 shows a missing mass analysis for a given incident photon energy and η polar angle. Coherent production events should be located around $E_{\text{MISS}} = 0$. Due to resolution effects quasifree events can, however, also contribute to this area. With no reasonable theoretical prediction for the shape of the quasifree background the fraction of coherent events can thus not be quantitatively determined. An upper limit can, however, be derived by fitting entries with $E_{\text{MISS}} > 0$ to the expected response function for a coherent signal (see Fig. 10). In Fig. 11 the upper limits with a significance of 1σ are shown

in comparison to three theoretical calculations. An improvement, albeit model dependent, could be made, if a better description for the quasifree mechanism could be provided.

4 Summary

It has been shown using inclusive and exclusive data that for quasifree η photoproduction from ^4He the ratio of the cross sections on bound neutrons and protons σ_n/σ_p is close to 2/3. This result agrees with other recent publications, where this value was deduced from inclusive measurements on the deuteron [2,4]. However, this verification does not solve the question with regard to the isospin structure of the electromagnetic excitation of the S_{11} resonance, but it implies that only an exclusive measurement of coherent η photoproduction from the deuteron can clarify the situation. Such an experiment has been performed using the same setup as this work and the analysis is currently in progress.

A new experiment to measure the coherent η photoproduction from ^3He is in preparation. It is part of the current TAPS program at MAMI. For ^3He , the quantum numbers ($S=1/2$, $I=1/2$) are most suitable for coherent η photoproduction involving the $S_{11}(1535)$ resonance. The cross section is expected to be much larger than on the deuteron and ^4He .

We wish to acknowledge the outstanding support of the accelerator group of MAMI, as well as many other scientists and technicians of the Institut für Kernphysik at the University of Mainz. This work was supported by Deutsche Forschungs-

gemeinschaft (SFB 201), Bundesministerium für Bildung und Forschung (BMBF, Contract No. 06 GI 475(3) I) and the UK Engineering and Physical Science Research Council.

References

1. B. Krusche et al., Phys. Rev. Lett. **74** (1995) 3736
2. B. Krusche et al., Phys. Lett. B **358** (1995) 40
3. M. Röbbig-Landau et al., Phys. Lett. B **373** (1996) 45
4. P. Hoffmann-Rothe et al., Phys. Rev. Lett. **78** (1997) 4697
5. A. Fix et al., Z. Phys. A **359** (1997) 427
6. H. Herminghaus, Proc. Linear Accelerator Conf. (Albuquerque, USA, 1990)
7. I. Anthony et al., Nucl. Instr. Meth. A **301** (1991) 230
8. R. Novotny, IEEE Trans. Nucl. Science **38** (1991) 379
9. R. Novotny et al., IEEE Trans. Nucl. Science **43** (1996) 1260
10. T.C. Awes et al., Nucl. Instr. and Meth. A **311** (1992) 130
11. M. Röbbig, diploma thesis, University of Gießen, unpublished, 1991
12. A.R. Gabler et al., Nucl. Instr. and Meth. A **346** (1994) 168
13. M. Kotulla, diploma thesis, University of Gießen, unpublished, 1997
14. McCarthy et al., Phys. Rev. C **15** (1977) 1396
15. R.P. Feynman et al., Phys. Rev. D **11** (1971) 2706
16. R. Koniuk and N. Isgur, Phys. Rev. D **21** (1980) 1886
17. Z. Li and F.E. Close, Phys. Rev. D **42** (1990) 2207
18. M. Warns et al., Phys. Rev. D **42** (1990) 2215
19. R. Bijker et al., Ann. of Phys. **236** (1994) 69
20. W.J. Metcalf and R.L. Walker, Nucl. Phys. B **76** (1974) 253
21. A. Fix et al., Nucl. Phys. A **620** (1997) 457
22. W. Peters et al., Nucl. Phys. A **640** (1998) 89
23. J. Piekarewicz et al., Phys. Rev. C **55** (1997) 2571